J. Mountain Res. P-ISSN: 0974-3030, E-ISSN: 2582-5011 DOI: https://doi.org/10.51220/jmr.v20-i2.19
Vol. 20(2), (2025), 154-165

Antimicrobial Activity and Characterisation of Biogenically Synthesised TiO_2 Nanoparticles Using Sea Buckthorn Fruit

Manoj Prasad Tamta [1] • Mahesh Chandra Vishwakarma [*1] • Balam Singh Bisht [2] • Pramod Singh Khati [3] • Rajesh Kumar [4] • Priyanka Tiwari [5] • Pradeep Durgapal [1]

[1] *Department of Chemistry, Govt Post Graduate College Berinag (Pithoragarh), Soban Singh Jeena University, Uttarakhand, India 262531*
[2] *HIMARC, Govt Post Graduate College Berinag (Pithoragarh), Soban Singh Jeena University, Uttarakhand, India 262531*
[3] *Department of Geology, DSB Campus, Kumaun University Nainital, Uttarakhand, India, 263001*
[4] *Department of Chemistry, Soban Singh Jeena University, Uttarakhand, India 262531*
[5] *Department of Chemistry, M.B. Govt Post Graduate College Haldwani (Nainital), Kumaun University Nainital, Uttarakhand, India 262531*

[*] Corresponding Author's email Id: mv.chandra4@gmail.com

Received: 21.09.2025; Revised: 30.11.2025; Accepted: 01.12.2025

Abstract: The green synthesis of metal or metal oxide nanoparticles using biogenic materials is a sustainable and environmentally friendly technique. In the present investigation, titanium dioxide nanoparticles (TiO_2NPs) were synthesised by using Sea buckthorn (*Hippophae salicifolia)* fruit (SBF) extract. The phytochemical extract of SBF served as both a reducing and stabilizing agent for the precursor. Optical and structural properties also indicated the successful formation of TiO_2NPs. UV–Vis absorption revealed a strong absorbance peak at 390 nm, with direct and indirect band gaps of 3.40 eV and 3.76 eV, respectively. The shape of the TiO_2NPs was crystalline anatase, as identified by XRD. The SEM micrographs revealed that the particles were irregular in shape, with an average size of ~85 nm. The EDS spectra revealed Ti and O as dominant elements. The FT-IR results stated the participation of hydroxyl, carbonyl, and phenolic groups from the fruit extract. The characteristic peak found at 670.80 cm^{-1} corresponds to Ti–O–Ti stretching vibrations. The antibacterial and antifungal activity of biosynthesized TiO_2NPs was determined against bacterial and fungal strains using the disc diffusion method. The zone of inhibition values against *Escherichia coli* and *Candida albicans* were 26.67 ± 0.58 mm and 15.67 ± 0.58 mm, respectively. The MICs of *Escherichia coli* and *Candida albicans* were 40 µg/mL and 60 µg/mL, respectively. The antimicrobial action is attributed to the production of reactive oxygen species (ROS) upon light exposure, which damages cell walls and induces ROS-mediated degradation of DNA and proteins. These results indicate that Sea buckthorn TiO_2NPs are potential candidates for antimicrobial applications.

Keywords: Sea buckthorn • Biogenic Synthesis • Characterisation • TiO_2NPs • Uttarakhand.

Introduction

Nanotechnology is an advanced, rapidly expanding field that investigates and manipulates materials at the atomic and molecular scale. Its emergence has transformed the development of nanostructures, enabling materials with enhanced and tailor-made properties (Kulkarni et al., 2023a). Among various nanomaterials, titanium dioxide (TiO_2), or titania, is a naturally occurring inorganic compound valued for its distinctive physicochemical characteristics. Titanium dioxide nanoparticles (TiO_2NPs) exist mainly in three crystalline phases—anatase, rutile, and brookite—with anatase and rutile being the most common and technologically relevant (Kose et al., 2020). These nanoparticles possess remarkable features such as a high refractive index, strong oxidising ability, chemical stability, and semiconductor behaviour, all of which make them highly useful in photocatalysis, environmental purification, medicine, food technology, and advanced materials research (Ul-Hamid et al., 2023a).

Metal oxide nanoparticles have drawn considerable global attention due to their multifunctional applications in sensors, biotechnology, electronics, cosmetics, pharmaceuticals, and energy systems (Murthy et al., 2020). Traditional approaches to nanoparticle synthesis, however, often rely on toxic reducing agents, high energy inputs, and costly procedures. These drawbacks have stimulated interest in green synthesis, an environmentally responsible and economically efficient alternative (Jamil et al., 2024). Green synthesis employs biological resources—particularly plants, bacteria, algae, and fungi—as reducing and stabilising agents. This method not only reduces chemical hazards but also offers improved biocompatibility and ecological sustainability (Kirubakaran et al., 2026). Plant-based synthesis is especially popular because plant extracts contain diverse phytochemicals and biopolymers capable of driving nanoparticle formation with controlled size, improved morphology, and enhanced photocatalytic activity (Khan et al., 2022). The anatase form of TiO_2 is particularly effective for photocatalytic applications. The efficiency of TiO_2NPs in environmental and antimicrobial applications largely depends on particle size, morphology, and surface area. Their high stability, non-toxicity, and strong oxidative capabilities make them excellent photocatalysts for wastewater treatment, microbial inhibition, and pollution control (Wellia et al., 2024).

Plants used in green synthesis provide rich phytochemical profiles that act simultaneously as reducing, capping, and stabilising agents governing nanoparticle characteristics. Sea buckthorn (*Hippophae salicifolia*), an important member of the Elaeagnaceae family, has gained particular interest as a promising biological source for nanoparticle synthesis. This hardy, nitrogen-fixing shrub thrives in diverse climates, especially in the Himalayan region and other temperate zones of Europe and Asia (Swenson & Bartish 2002). Traditionally regarded as the "Wonder Plant" or "Golden Bush," sea buckthorn is valued for its extensive nutritional, medicinal, and ecological uses (Chen et al., 2023). Its fruits, leaves, and seeds contain a wide range of bioactive compounds, including flavonoids, carotenoids, phenolic acids, phytosterols, amino acids, vitamins, and essential fatty acids. Notably, the berries are exceptionally rich in antioxidant compounds such as rutin, myricetin, isorhamnetin, tocopherols, and carotenoids (Ren et al., 2020). Sea buckthorn also provides high levels of vitamins C and E, polyunsaturated fatty acids, triterpenoids, organic acids, and sterols, all of which contribute to its therapeutic and antimicrobial activities (Kubczak et al., 2022). These phytochemicals actively participate in the reduction and stabilisation of metal nanoparticles, enhancing their structural and functional characteristics.

In the present study, titanium dioxide nanoparticles were synthesised using a green method in which the fruit extract of *Hippophae salicifolia* served as both reducing and stabilising agent. The synthesised TiO_2NPs were extensively characterised using a suite of analytical techniques. UV–visible spectroscopy was used to examine optical properties and estimate the band gap, while X-ray diffraction (XRD) was employed to confirm crystallinity and calculate crystallite size. Scanning electron microscopy (SEM) and energy-dispersive X-ray spectroscopy (EDS) provided insights into morphology and elemental composition, whereas transmission electron microscopy (TEM) offered high-resolution visualisation of shape and particle size. Fourier-transform infrared spectroscopy (FTIR) identified the functional groups responsible for nanoparticle capping, confirming successful biosynthesis. The antimicrobial activity of the biosynthesised TiO_2NPs was evaluated against Pseudomonas aeruginosa and Escherichia coli, and antifungal efficacy was tested against Candida parapsilosis, Candida tropicalis, and Candida albicans using disc diffusion and minimum inhibitory concentration (MIC) assays.

Materials and Methods

Required Material: Titanium Tetra Isopropoxide (TTIP) (27.8-28.6% Purity), was used as an analytical-grade reagent without any further processing. Samples for dehydration, a hot air oven, and a muffle furnace are required; then a magnetic stirrer is compulsory for this reaction.

Collection of Plant: Sea buckthorn fruit was collected from an open forest site of the Nature and Education Eco Park Centre, Munsyari, Pithoragarh, Uttarakhand, India. The fruits were rinsed with double-distilled water to eliminate dust and adherent particles. The fruits were washed and then squeezed into small pieces for extraction.

Preparation of Plant Extract: Weigh 50 g of the Fruits of the plant in a 500 ml beaker. Filter the mixture using Whatman 42 filter paper after boiling the mixture at 70^0C for one hour. Filtrate is taken for subsequent experiments.

Green synthesis of Titanium dioxide nanoparticles: Add 25 mL of titanium tetra-isopropoxide to a 500 mL beaker. Then, dropwise and stir the titanium tetra isopropoxide solution with 20 mL of (SBF) extract. The mixture is then stirred for 2 hours at room temperature. Through this process, the colour changes from white to a yellowish-gray, indicating that titanium dioxide nanoparticles have been successfully formed. The solution is filtered, and the samples are kept in an oven at 110°C for 5 hours. Eventually, the samples are dried and calcined at 500°C in a muffle furnace for 2 hours.

Evaluation of Antimicrobial Activity

Disc diffusion assay: The antimicrobial effect of TiO_2NPswas measured using the disc diffusion technique. 10-µL of TiO_2NPs suspensions at various concentrations were impregnated into sterile filter paper discs (6 mm) and deposited on inoculated Mueller–Hinton agar (bacterial) and on Savoured dextrose agar (fungi) plates. The suspension was standardized to 0.5 McFarland (~10^8 CFU/ml). As positive controls, Ciprofloxacin (5 µg/disc) and Amphotericin B (10 µg/disc) were used, while negative control discs were loaded only with distilled water. Plates were then incubated at 37 °C for 24 h (bacteria) and 28 °C for 48 h (fungi). Diameters of zones of inhibition (ZOI) were recorded in mm(Rahaman et al. 2020).

MIC determination: MICs were obtained by broth microdilution (10–100 µg/mL). The MIC was determined as the lowest concentration at which no visible growth was observed.

Statistics: All experiments were conducted at least three times (n = 3). Means are presented ± SD. Chi-square, RMS, χ^2, and P values are provided ($P < 0.05$ was considered significant).

Characterisation of TiO_2NPs: A comprehensive range of advanced characterization techniques was employed to characterize the synthesized titanium dioxide nanoparticles (TiO_2NPs) from the Sea buckthorn *(Hippophae salicifolia)* fruit extract. The methods employed were UV-Vis spectroscopy (λ = 750, Labtronics Model LT-29), X-ray diffraction (Rigaku miniflex 600), Fourier transform infrared spectroscopy (PerkinElmer Spectrum IR Version 10.7.2), Scanning Electron Microscopy (SEM), and Energy-Dispersive X-ray Spectroscopy (EDS) (Carl Zeiss EVO 18 with EDAX). Characterization techniques include XRD to assess the crystallinity and purity of the nanoparticles, as well as UV-Vis spectroscopy to study their optical properties. Various chemical bonds were identified by FT-IR spectroscopy, whereas the particle size and morphology were characterized by SEM with JIMAGE software. XRD characterization confirmed the formation of TiO_2NPs, whereas EDS analysis provided details of their elemental composition. Moreover, transmission electron microscopy (TEM) analysis of the green-synthesized nanoparticles also provided valuable insights into their morphology, nanoparticle size, and crystalline structure.

Results and Discussion

Characterisation of green Synthesised TiO_2NPs using SBF extract

UV-Vis Spectroscopy: UV-Visible spectroscopy was used to examine the optical absorption characteristics of the biosynthesised TiO_2NPs (Fig. 2). The absorption spectrum indicated a very sharp absorption peak at approximately 390 nm, a characteristic value of TiO_2NPs. This is an abrupt absorption in the UV range due to the electronic transition between the conduction and valence bands(Rathore et al. 2023).

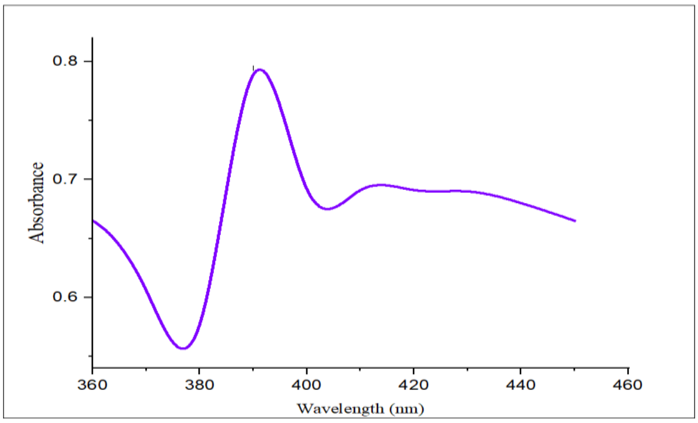

Fig. 2: UV–Vis absorption spectrum of biosynthesized TiO_2NPs.

The optical band gap energy, Eg, was determined using the Tauc relation.

$$(\alpha h\nu)^{1/n} = A(h\nu - E_g) \quad \ldots(1)$$

where α (alpha) represents the absorption coefficient, h is Planck's constant, A is absorbance, E_g is band gap energy, ν frequency of band gap, and n is an exponent that describes the nature of the electronic transition. n = 1/2 for a direct allowed transition and n = 2 for an indirect allowed transition.

The $(\alpha h\nu)^2$ vs hν plot showed that the direct band gap was 3.50 eV, whereas the $(\alpha h\nu)^{1/2}$ vs hν plot showed that the indirect band gap was 3.90 eV. These values are slightly larger than those of bulk TiO_2 (3.2 eV), indicating a blue shift, which is a quantum confinement effect on the nanoscale (Einert et al. 2021). The values of the absorption and band gap, as observed, support the fact that the synthesised TiO_2NPs possess high optical

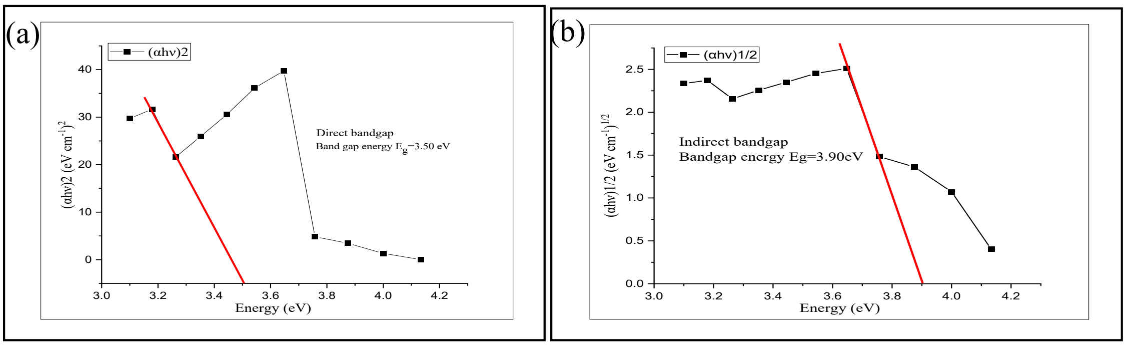

Fig. 3: Tauc plots of biosynthesized TiO_2NPs (a) direct band gap, and (b) indirect band gapX-ray Diffraction (XRD):

The crystalline nature and phase identification of the biosynthesized TiO_2NPs using Sea buckthorn fruit extract were confirmed by X-ray diffraction (XRD) analysis. The XRD pattern (Fig. 4) shows several sharp and intense diffraction peaks, indicating the formation of crystalline nanoparticles. The major diffraction peaks were observed at 2θ values around 25.3°, 37.8°, 48.0°, 54.0°, 55.1°, 62.6°, 68.8°, 70.3° and 75.0°, which

 DOI: https://doi.org/10.51220/jmr.v20-i2.19

correspond to the (101), (004), (200), (105), (211), (204), (116), (220), and (215) crystal planes of TiO_2NPs. These planes are in good agreement with the standard JCPDS card No. 21-1272, confirming the anatase phase of TiO_2(Asadzadeh Patehkhor et al. 2021). The strong and sharp diffraction peak at 25.3° (101) plane is characteristic of the anatase phase, which is known for its high photocatalytic activity. The absence of secondary peaks corresponding to rutile or brookite phases suggests that the synthesized TiO_2NPs are predominantly anatase in nature. The narrow and intense peaks indicate high crystallinity of the nanoparticles (Azeez et al., 2018). The average crystallite size (D) of the TiO_2NPs can be estimated using the Debye–Scherrer equation:

$$D = \frac{K\lambda}{\beta \cos \theta} \quad \text{......(2)}$$

where K is the shape factor (0.9), λ is the X-ray wavelength (1.5406 Å for Cu Kα radiation), β is the full width at half maximum (FWHM) of the most intense peak (in radians), and θ is the Bragg's angle. Based on the most intense (101) diffraction peak, the average crystallite size was calculated to be in the range of 15–25 nm, indicating nanoscale dimensions (Londoño-Restrepo et al. 2019). These results confirm that the Sea buckthorn fruit extract not only acted as a reducing agent but also as a stabilizing agent in the green synthesis process, leading to the formation of highly crystalline anatase TiO_2NPs. The biosynthesized TiO_2NPs with a smaller crystallite size and higher crystallinity are expected to exhibit enhanced photocatalytic and antimicrobial activities (Sagadevan et al. 2021).

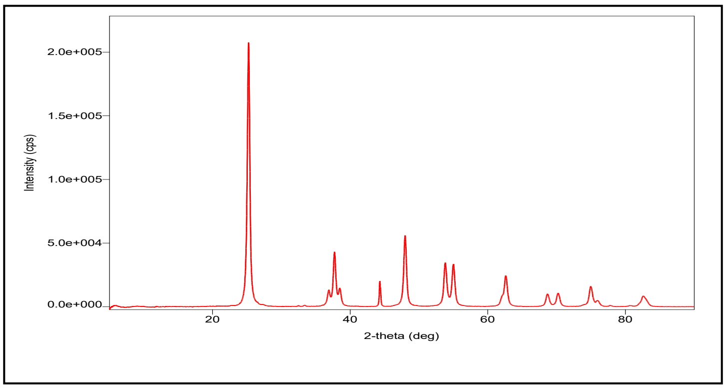

Fig. 4: XRD diffractogram of TiO_2NPs synthesized using Sea buckthorn.

Scanning Electron Microscope Energy Dispersive X-ray (SEM-EDS): Scanning electron microscopy (SEM) was used to examine the surface morphology of biosynthesized TiO_2NPs using *Hippophae salicifolia* (sea buckthorn) extract. The SEM micrograph (Fig. 5) shows that the nanoparticles are mostly spherical to almost spherical in shape. There is some agglomeration, which is common in plant-mediated synthesis, because phytochemicals act as reducing and stabilising agents (López-Mercado et al. 2023b). The micrograph shows that the particles were approximately 67–101 nm in size, which falls within the nanometre range. The average particle size is approximately 85 nm. The small difference in size is due to the natural reducing and capping agents in the plant extract, which control nucleation and growth, but may also cause mild aggregation (Zulfiqar et al. 2019). Even though the nanoparticles are clumped together, it is still possible to see each one, indicating that TiO_2 was successfully synthesised at the nanoscale (Aslam et al., 2021). The morphology indicates that the sea buckthorn fruit extract effectively reduced titanium precursors and stabilized the resulting nanoparticles, thereby creating nanostructures

 DOI: https://doi.org/10.51220/jmr.v20-i2.19

of optimal dimensions for potential antibacterial applications (Aslam et al., 2021).

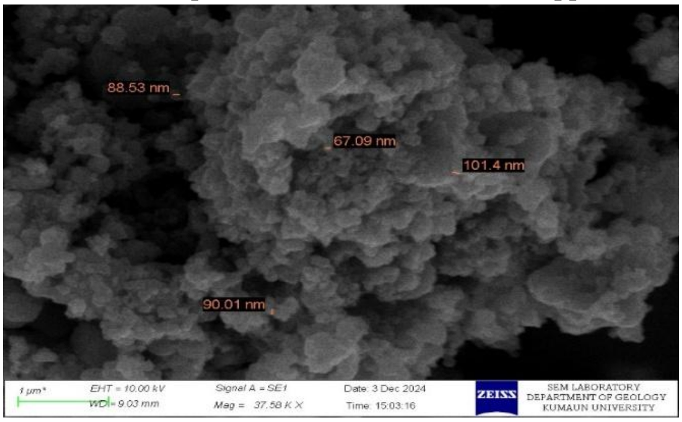

Fig. 5: SEM image of Green synthesised TiO_2NPs using Sea buckthorn fruit extract

The energy-dispersive X-ray spectroscopy (EDS) to determine the elemental composition of the biosynthesised TiO_2NPs. The spectra obtained (Fig. 6) distinctly display the characteristic peaks for titanium (Ti) and oxygen (O), confirming the synthesis of titanium dioxide nanoparticles. The pronounced oxygen peak at approximately 0.5 keV and the distinct titanium peaks at around 4.5 and 4.9 keV further substantiate that TiO_2 possesses a stoichiometric composition (Atique Ullah et al. 2019a). In addition to titanium (Ti) and oxygen (O), minor peaks of carbon (C) and nitrogen (N) were also detected. The peaks may result from the organic compounds included in the SBF extract utilised in the green synthesis process. These biomolecules often serve as reducing and stabilising agents, resulting in the capping of the nanoparticle surface. The presence of Au signals in the spectrum is attributable to the sample being coated with Gold to enhance its conductivity before the SEM analysis (Bharadwaj et al. 2021). The prominence of the Ti and O peaks in the spectrum indicates the purity of the nanoparticles. The additional bio-originated signals (C and N) indicate that plant metabolites effectively engaged with the nanoparticle surface. This type of organic functionalization enhances the stability and biocompatibility of nanoparticles for biological applications (Atique Ullah et al. 2019a).

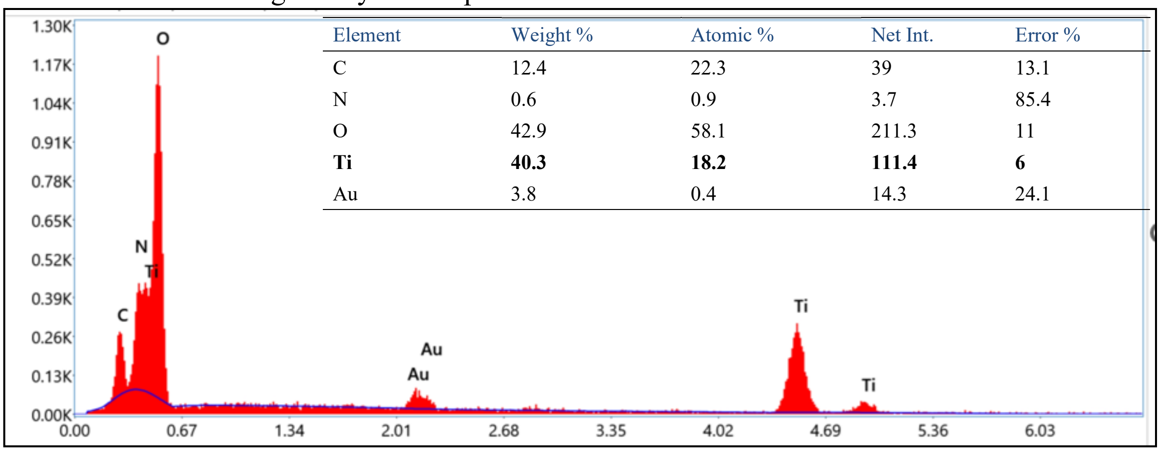

Element	Weight %	Atomic %	Net Int.	Error %
C	12.4	22.3	39	13.1
N	0.6	0.9	3.7	85.4
O	42.9	58.1	211.3	11
Ti	**40.3**	**18.2**	**111.4**	**6**
Au	3.8	0.4	14.3	24.1

Fig. 6: EDS Spectrum of Green synthesised TiO_2NPs using Sea buckthorn fruit extract.

Transmission electron microscopy (TEM): Transmission Electron Microscopy (TEM) was used to study the morphology and average particle size of the biosynthesised TiO_2NPs. TEM micrographs exhibited nearly spherical to quasi-spherical particles with minor agglomeration, as per the common nature of phyto-synthesised nanoparticles owing to the capping biomolecules. The particle size distribution measured an average diameter of 129.85 nm (standard deviation: SD = 42.556 nm), confirming the nanoscale nature and polydispersity of the sample (Mohany et al. 2023). TEM particle size was somewhat larger than the 15–25nm calculated crystallite size determined from XRD. This variation occurs because while XRD measures the crystallite size (single crystal domain), TEM measures the particle size, including aggregated crystallites and organic capping from Sea buckthorn fruit extract. This fact is also confirmed by SEM images, which show the aggregated structure of nanoparticles with an average size of ≈approximately 85 nm (Saka et al. 2022). Generally, TEM study substantiates that nano-TiO_2NPs were synthesized as nanomaterials with a relatively uniform structure (homogeneous) and morphology, confirming that the Sea buckthorn fruit extract-mediated synthesis was successful (Atique Ullah et al. 2019b).

Fig 7: (a) **Green synthesised TiO_2NPs (a) TEM micrograph with partial aggregation; (b) particle size distribution histogram**

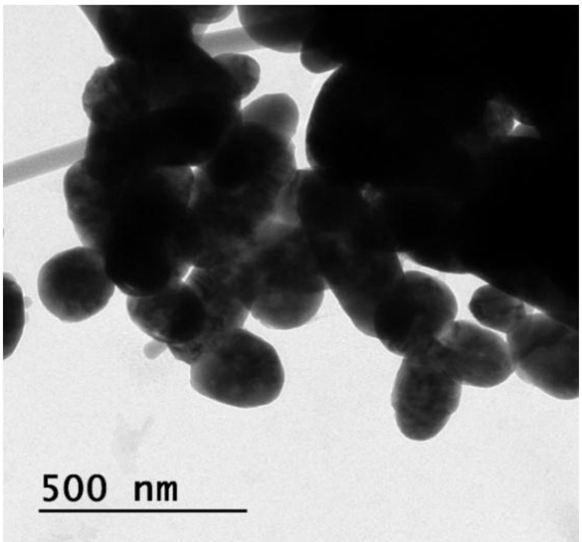

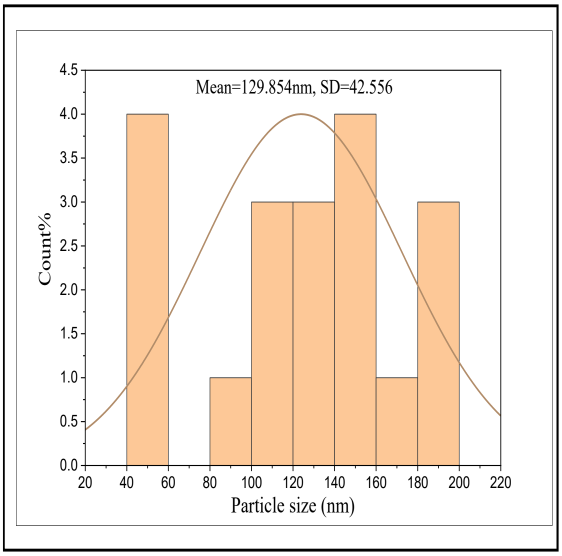

FT-IR: The FTIR spectrum of the Sea buckthorn fruit extract-mediated TiO_2NPs is illustrated in (Fig. 8). Several absorption bands between 4000 and 400 cm⁻¹, which show that biomolecules from the fruit extract were involved in making and stabilizing TiO_2NPs (Tasisa et al. 2025). A broad band at 3737.45 cm^{-1} and 3649.84 cm^{-1} is due to the O–H stretching vibrations of hydroxyl groups found in alcohols, phenols, or absorbed water molecules. This suggests that they help stabilize nanoparticles. The absorption peaks at 2981.54 cm^{-1} and 2889.54 cm^{-1} correspond to C–H stretching vibrations of aliphatic $–CH_2$ groups, indicating the presence of organic compounds from the extract on the surface of the nanoparticles (Nguyen et al. 2022). The band at 1382.16 cm^{-1} is due to C–N stretching vibrations of amines or bending vibrations of phenolic –OH groups. The peak at 1250.84 cm^{-1} is due to C–O stretching vibrations of alcohols, esters, or carboxylic acids. C–O–C vibrations are linked to a specific absorption near 1152.43 cm^{-1}. This shows that flavonoids, polysaccharides, and other phytochemicals are involved in the capping process(Shahzad Shirazi et al. 2022). The most important observation is that the unique strong absorption band at 670.80 cm^{-1} corresponds to Ti–O–Ti stretching vibrations, indicating that TiO_2NPs have formed (Atique Ullah et al. 2019c).

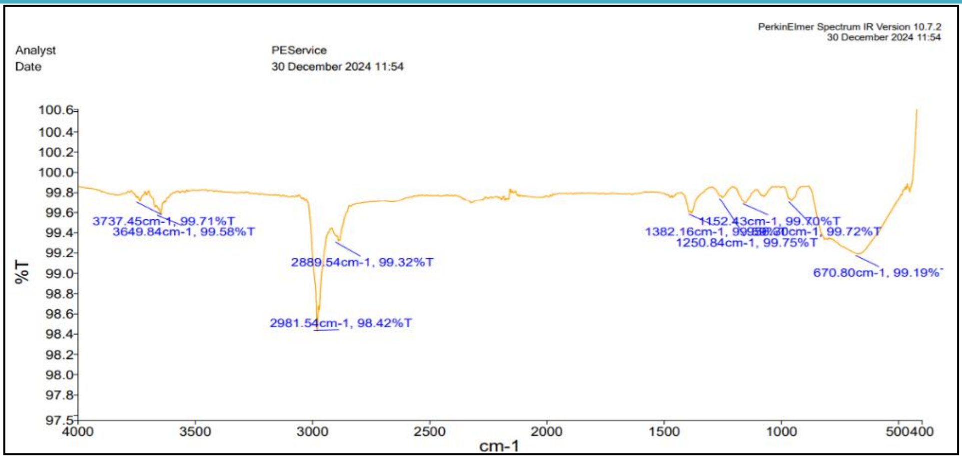

Fig. 8: FT-IR Spectrum of Green Synthesised TiO_2NPs Using Sea buckthorn fruit

FTIR analysis confirms that biomolecules present in Sea buckthorn fruit extract, including polyphenols, flavonoids, proteins, and organic acids, play a role in reducing the Ti precursor and maintaining the stability of the nanoparticles. These biomolecules not only facilitated the green synthesis process but also enhanced the stability of the biosynthesized TiO_2NPs by preventing them from clumping together (Aslam et al. 2021b).

Antimicrobial Activity: The antibacterial and antifungal potential of the TiO_2NPs using Sea buckthorn fruit extract was screened using the disc diffusion method against two bacteria (*E. coli, P. aeruginosa*) and three fungi (*C. albicans, C. tropicalis*, and *C. parapsilosis*). These results are presented in Table 2 and Fig. 9. The *E. coli* were also found to be highly vulnerable in the presence of TiO_2NPs, as indicated by the ZOI (26.67 ± 0.58 mm), which was very similar to that of the positive control Ciprofloxacin (33 mm). The inhibition zone was slightly wider than the control; however, it was still markedly diminished (χ^2 = 10.0; p < 0.02), confirming an intense antimicrobial effect of TiO_2NPs on Gram-negative bacteria. The nanoparticles demonstrated mild antifungal activity on *C. albicans* with 15.67 ± 0.58 mm ZOI, when compared to the positive control, Amphotericin B (12 mm). The difference was not significant (χ^2 = 2.0; p = 0.15), but a trend was detected, indicating intermediate antifungal action.

Table: 2 ZOI and Statistical Evaluation of TiO_2NPs against different pathogens

SN	Organism	ZOI ± SD (mm)	Positive Control (PC)	PC Zone (mm)	χ^2	RMS	p-value	Significance
1	*E. coli*	26.67 ± 0.58	Ciprofloxacin	33	10	6.3	0.02	Significant
2	*P. aeruginosa*	0.00 ± 0.00	Ciprofloxacin	23				Not detected
3	*C. tropicalis*	0.00 ± 0.00	Amphotericin B	10.33				Not detected
4	*C. parapsilosis*	0.00 ± 0.00	Amphotericin B	12				Not detected
5	*C. albicans*	15.67 ± 0.58	Amphotericin B	12	2	3	0.15	Moderate

Nevertheless, no inhibition zones were observed in front of *P. aeruginosa, C. tropicalis*, and *C. parapsilosis* (these yeasts showed to be more resistant to TiO_2NPs action). The reason it was inactive against *P. aeruginosa*, a bacterium with significant intrinsic resistance and the ability to form biofilms for its protection, may be very strong. The absence of activity against Fungi (except *C. albicans*) could depend on the construction of the cell wall and the resistance process.

Minimum Inhibitory Concentration (MIC): MIC determination by the broth microdilution method also validated the ZOI measurements

(Table 3, Fig. 10 Visible microbial growth of *E. coli* could be completely inhibited at 40 µg/mL, and that of *C. albicans* when the drugs were tested at 60 µg/mL. These data are in accordance with MIC values previously described for biogenic TiO_2NPs, which range between 25 µg/mL and 100 µg/mL, depending on the microorganism strain and synthesis conditions.

Table: 3 MIC and Statistical Evaluation of TiO_2NPs against different pathogens

Pathogen	***E. coli***	***P. aeruginosa***	***C. tropicalis***	***C. parapsilosis***	***C. albicans***
MIC (µg/mL)	40	–	–	–	60

Notably, *C. albicans* had a higher MIC than that of *E. coli*, indicating that bacterial cells are more susceptible to ROS than yeast cells. Its thicker chitin-glucan cell walls and stronger antioxidant defense system of fungal pathogens could contribute to higher MICs found with *C. albicans*.

The MIC of *P. aeruginosa, C. tropicalis,* and *C. parapsilosis* was not determinable, in agreement with the lack of ZOI in the disc diffusion test.

Mechanism of Antimicrobial Activity: The antimicrobial activity of TiO_2NPs synthesised using Sea buckthorn fruit extract can be explained by their photocatalytic properties and the generation of reactive oxygen species (ROS).

Photoexcitation across the band gap: The antimicrobial activity of Sea buckthorn-mediated TiO_2NPs begins with photoexcitation. When exposed to light, electrons in the valence band are excited to the conduction band, leaving behind positively charged holes. The process generates electron–hole (e^-/h^+) pairs on the nanoparticle surface, which serve as active sites for subsequent redox reactions.

When light energy ≥ their band gap hits TiO2, electrons (e^-) excite from the valence band (VB) to the conduction band (CB), leaving holes (h^+) in the VB.

Generation of reactive oxygen species (ROS): Photoexcited electron–hole pairs engage in surface redox reactions producing reactive oxygen species (ROS). Excited electrons reduce O_2 to superoxide anions (O_2^{-}•), and holes oxidize water or hydroxide ions to hydroxyl radicals (•OH). Singlet oxygen and hydrogen peroxide may also form as secondary ROS, creating a highly oxidative environment around the nanoparticles.

These photo-generated charge carriers drive redox reactions on the nanoparticle surface, leading to the production of ROS (Seiß et al. 2021).

Step 1 Reduction (Conduction Band):

$$e^-_{(CB)} + O_2 \longrightarrow O_2^{\cdot} + H^+ \longrightarrow 2HO_2^{\cdot} \longrightarrow H_2O_2 + O_2 \longrightarrow 2^{\cdot}OH$$

Step 2 Oxidation Reactions (Valence Band):

$$h^+_{(VB)} + H_2O \longrightarrow {}^{\cdot}OH + H^+$$

$$h^+_{(VB)} + OH^- \longrightarrow {}^{\cdot}OH$$

The cumulative oxidative stress overwhelms microbial defence systems, resulting in cell death (Ikram et al. 2020).

ROS-mediated biomolecular damage: The reactive oxygen species generated by the nanoparticles exert strong oxidative effects on microbial cellular components. ROS attack the lipid bilayer of the cell membrane, causing increased permeability and ultimately leading to structural disintegration. Proteins are oxidised, leading to enzyme inactivation and impaired cellular functions. Furthermore, ROS induce damage to nucleic acids through strand breaks and base modifications, thereby interfering with replication and transcription processes.

Irreversible oxidative stress and cell death: Reactive oxygen species (ROS) overload causes irreversible oxidative stress, damaging cell membranes, proteins, and DNA, leading to microbial death. This explains the potent antimicrobial activity of Sea buckthorn-mediated TiO_2NPs.

Conclusion

The study demonstrated green synthesis of TiO_2NPs using Sea buckthorn extract as a reducing and stabilising agent. Characterisation showed structural, morphological, and functional properties, including a 390 nm absorption edge, a direct band gap of 3.50 eV, and an indirect band gap of 3.90 eV, indicating quantum confinement. Crystalline anatase phase particles ranged from 15–85 nm, stabilised by phytochemicals acting as capping agents, confirmed by FT-IR and Ti–O–Ti vibrations. Biosynthesised TiO_2NPs showed selective antimicrobial activity, strongly inhibiting E. coli (MIC 40 µg/mL) and moderately inhibiting C. albicans (MIC 60 µg/mL), via light-induced ROS causing cell wall and biomolecular damage. The results showcase Sea buckthorn-mediated TiO_2NPs as eco-friendly antimicrobial nanomaterials with potential in biomedical, pharmaceutical, and environmental applications. Future research should explore photocatalytic uses.

References

Asadzadeh Patehkhor H, Fattahi M and Khosravi-Nikou M (2021) 'Synthesis and characterization of ternary chitosan–TiO2–ZnO over graphene for photocatalytic degradation of tetracycline from pharmaceutical wastewater', *Sci Rep*, **11**, p.p. 24177–24188

Aslam M, Abdullah AZ and Rafatullah M (2021a) 'Recent development in the green synthesis of titanium dioxide nanoparticles using plant-based biomolecules for environmental and antimicrobial applications', *Journal of Industrial and Engineering Chemistry*, **98**, p.p. 1–16

Atique Ullah AKM, Tamanna AN, Hossain A, Al-Ani L, Noman M, Khan R, Saeed A, Zaman S, Ali M and Farooq U (2019a) 'In vitro cytotoxicity and antibiotic application of green route surface modified ferromagnetic TiO_2NPs', *RSC Adv*, **9**, p.p. 13254–13262

Azeez F, Al-Hetlani E, Arafa M, El-Din MA, Al-Othman ZA, Al-Mutairi K, Al-Qahtani S, Alharbi H, Al-Rashidi I and Al-Faifi N (2018b) 'The effect of surface charge on photocatalytic degradation of methylene blue dye using chargeable titania nanoparticles', *Sci Rep*, **8**, p.p. 7104–7116

Bharadwaj KK, Rabha B, Pati S, Gogoi BK, Borgohain P, Das S, Choudhury R, Deka S, Kalita D and Sharma A (2021) 'Green Synthesis of Gold Nanoparticles Using Plant Extracts as Beneficial Prospect for Cancer Theranostics', *Molecules*, **26**, p.p. 6389–6405

Chen Y, Cai Y, Wang K and Wang Y (2023) 'Bioactive Compounds in Sea Buckthorn and their Efficacy in Preventing and Treating Metabolic Syndrome', *Foods*, **12**, p.p. 1985–2000

Einert M, Hartmann P, Smarsly B and Brezesinski T (2021) 'Quasi-homogenous photocatalysis of quantum-sized Fe-doped TiO2 in optically transparent aqueous dispersions', *Sci Rep*, **11**, p.p. 17687–17700

Ikram M, Umar E, Raza A, Khan M, Ali S, Ali Q, Ahmed S, Khan H, Asif M and Shahid M (2020) 'Dye degradation performance, bactericidal behavior and molecular docking analysis of Cu-doped TiO2NPs', *RSC Adv*, **10**, p.p. 24215–24233

Jamil YMS, Al-Hakimi AN, Al-Maydama HMA, Hassan MM, Al-Malki FA, Alhassan S, Al-Akhras MA, Alotaibi MA, Alsubaie AM and Alhajri RA (2024) 'Optimum Green Synthesis, Characterisation, and Antibacterial Activity of Silver Nanoparticles

Prepared from an Extract of Aloe fleurentinorum', *International Journal of Chemical Engineering*, **2024**, p.p. 1–15

Khan F, Shariq M, Asif M, Ali S, Umar E, Raza A, Ikram M, Khan M, Rehman A and Hassan A (2022) 'Green Nanotechnology: Plant-Mediated Nanoparticle Synthesis and Application', *Nanomaterials*, **12**, p.p. 673–690

Kirubakaran D, Wahid JBA, Karmegam N, Subramani R, Nallusamy S, Kumar G, Rajendran S, Selvaraj R, Ramkumar S and Ramesh S (2026) 'A Comprehensive Review on the Green Synthesis of Nanoparticles: Advancements in Biomedical and Environmental Applications', *Biomedical Materials & Devices*, **4**, p.p. 388–413

Kose O, Tomatis M, Leclerc L, Rossi F, Guarneri A, Bianchi A, Martinelli G, Silva P, Fernandez R and Kumar S (2020) 'Impact of the Physicochemical Features of TiO_2NPs on Their In Vitro Toxicity', *Chem Res Toxicol*, **33**, p.p. 2324–2337

Kubczak M, Khassenova AB, Skalski B, Janczak D, Nowak A, Szymczak M, Wójcik M, Górski A, Piekarska A and Kowalski R (2022) 'Hippophae *salicifolia* L. leaf and twig extracts as rich sources of nutrients and bioactive compounds with antioxidant activity', *Sci Rep*, **12**, p.p. 1095–1108

Kulkarni D, Sherkar R, Shirsathe C, Patil S, Pawar P, Deshmukh P, Jadhav S, More S, Shinde R and Waghmare S (2023a) 'Biofabrication of nanoparticles: sources, synthesis, and biomedical applications', *Front Bioeng Biotechnol*, **11**, p.p. 1–20

Londoño-Restrepo SM, Jeronimo-Cruz R, Millán-Malo BM, Sánchez-Ruiz F, Torres-Rojas C, Lopez-Moreno J, Guzmán-Méndez A, Molina-Rivera L, Estrada-Garcia M and Paredes-Lopez O (2019) 'Effect of the Nano Crystal Size on the X-ray Diffraction Patterns of Biogenic Hydroxyapatite from Human, Bovine, and Porcine Bones', *Sci Rep*, **9**, p.p. 5915–5928

López-Mercado J, González-Domínguez MI, Reynoso-Marin FJ, Pérez-Sánchez F, Mendoza-Castillo D, López-Castillo D, García-Ramos J, Ramírez-González A, Hernández-Sánchez H and Torres-Martínez L (2023b) 'Green synthesis of TiO2 for furfural production by photohydrolysis of tortilla manufacturing waste', *Sci Rep*, **13**, p.p. 15355–15370

Murthy S, Effiong P and Fei CC (2020) 'Metal oxide nanoparticles in biomedical applications', In: *Metal Oxide Powder Technologies*, Elsevier, p.p. 233–251

Nguyen THA, Nguyen VC, Phan TNH, Tran QH, Le TM, Hoang NM, Bui TT, Pham HT, Nguyen TN and Doan T (2022) 'Novel biogenic silver and gold nanoparticles for multifunctional applications: Green synthesis, catalytic and antibacterial activity, and colorimetric detection of Fe(III) ions', *Chemosphere*, **287**, p.p. 132271–132285

Rahaman MS, Siraj MA, Sultana S, Alam M, Hasan M, Khan R, Akhtar S, Islam N, Hossain M and Chowdhury A (2020) 'Molecular Phylogenetics and Biological Potential of Fungal Endophytes From Plants of the Sundarbans Mangrove', *Front Microbiol*, **11**, p.p. 1–15

Rathore C, Yadav VK, Gacem A, Sharma P, Singh A, Kumar R, Khan M, Gupta S, Patel D and Mehta R (2023) 'Microbial synthesis of titanium dioxide nanoparticles and their importance in wastewater treatment and antimicrobial activities: a review', *Front Microbiol*, **14**, p.p. 1–18

Ren R, Li N, Su C, Zhao L, Wang H, Chen X, Zhang Y, Liu Q, Huang Y and Xu J

(2020) 'The bioactive components as well as the nutritional and health effects of sea buckthorn', *RSC Adv*, **10**, p.p. 44654–44671

Sagadevan S, Anita Lett J, Vennila S, Murugan B, Imteyaz S, Kumar P, Reddy AV, Jayarambabu N, Shanmugam A and Rajeshkumar S (2021) 'Photocatalytic activity and antibacterial efficacy of titanium dioxide nanoparticles mediated by Myristica fragrans seed extract', *Chem Phys Lett*, **771**, p.p. 138527–138536

Saka A, Shifera Y, Jule LT, Tadesse M, Desta H, Mekonnen B, Alemayehu A, Kassa A, Tesfaye D and Bekele T (2022) 'Biosynthesis of TiO_2NPs by Caricaceae (Papaya) shell extracts for antifungal application', *Sci Rep*, **12**, p.p. 15960–15972

Seib V, Helbig U, Lösel R and Eichelbaum M (2021) 'Investigating and correlating photoelectrochemical, photocatalytic, and antimicrobial properties of TiO2 nanolayers', *Sci Rep*, **11**, p.p. 22200–22212

Shahzad Shirazi M, Moridi Farimani M, Foroumadi A, Ghiasvand A, Hemmati M, Asghari M, Sadeghi H, Ahmadi F, Ramezani M and Najafi F (2022) 'Bioengineered synthesis of phytochemical-adorned green silver oxide (Ag2O) nanoparticles via Mentha pulegium and Ficus carica extracts with high antioxidant, antibacterial, and antifungal activities', *Sci Rep*, **12**, p.p. 21509–21522

Swenson U and Bartish IV (2002) 'Taxonomic synopsis of Hippophae (Elaeagnaceae)', *Nord J Bot*, **22**, p.p. 369–374

Ul-Hamid A, Baig N, Haider A, Qureshi Z, Ahmed S, Khan R, Malik M, Ali F, Hussain T and Khan I (2023a) 'Using biologically synthesized TiO_2NPs as potential remedy against multiple drug resistant Staphylococcus aureus of bovine mastitis', *Sci Rep*, **13**, p.p. 18785–18796

Wellia DV, Syuadi AF, Rahma RM, Nugroho A, Putra D, Wibowo T, Hadiyanto H, Santoso P, Prasetyo A and Utomo R (2024) 'Rind of Aloe vera (L.) Burm. f extract for the synthesis of titanium dioxide nanoparticles: Properties and application in model dye pollutant degradation', *Case Studies in Chemical and Environmental Engineering*, **9**, p.p. 100627–100638

Zulfiqar H, Zafar A, Rasheed MN, Khan R, Ali S, Ahmed F, Hussain T, Malik M, Riaz M and Tariq F (2019) 'Synthesis of silver nanoparticles using Fagonia cretica and their antimicrobial activities', *Nanoscale Adv*, **1**, p.p. 1707–1713